The 3D Galactocentric velocities of Kepler stars: marginalizing over missing RVs

Ruth Angus,[1,2] Adrian M. Price-Whelan,[2] Dan Foreman-Mackey,[2] Joel Zinn,[3] and Megan Bedell[2]

[1]*Department of Astrophysics, American Museum of Natural History, 200 Central Park West, Manhattan, NY, USA*
[2]*Center for Computational Astrophysics, Flatiron Institute, 162 5th Avenue, Manhattan, NY, USA*
[3]*NSF Fellow, Department of Astrophysics, American Museum of Natural History, 200 Central Park West, Manhattan, NY, USA*

ABSTRACT

The three-dimensional velocities of stars can reveal their orbital properties and their kinematic ages. Precise Gaia measurements of positions, parallaxes and proper motions provide an opportunity to measure the two-dimensional velocities of billions of Galactic stars. Radial velocity (RV) measurements from spectroscopic surveys provide an opportunity to calculate three-dimensional velocities for some of these stars. Gaia will provide RVs for stars as faint as 15th magnitude in its third data release, however there are now and will remain many stars without RV measurements. Without RV measurements, it is still possible to infer full three-dimensional velocities by marginalizing over the missing RV dimension. In this paper, we infer the three-dimensional velocities of stars in the Kepler field in Galactocentric coordinates ($v_\mathbf{x}$, $v_\mathbf{y}$, $v_\mathbf{z}$). Lying at a low galactic latitude, the Kepler field is oriented close to the y-axis of the Galactocentric coordinate system. Without RVs, this means that $v_\mathbf{y}$ is poorly constrained, but $v_\mathbf{x}$ and $v_\mathbf{y}$ can still be precisely inferred. For many applications, including kinematic age-dating, having precise velocities in the $v_\mathbf{z}$ and $v_\mathbf{x}$ directions are sufficiently useful. This method, applied in different parts of the sky, will result in a different mix of precision distributed across the $v_\mathbf{x}$, $v_\mathbf{y}$, and $v_\mathbf{z}$ dimensions. However, although our methodology is broadly applicable to targets across the sky, our prior is specifically constructed from and for the Kepler field. Care should be taken therefore, when applying this method to other parts of the Galaxy, that a suitable prior is used.

Keywords: Milky Way Dynamics

1. INTRODUCTION

Gaia has revolutionized the field of Galactic dynamics by providing precise positions and proper motions for an unprecedented number of stars in the Milky Way. So far, Gaia has provided positions and proper motions for billions of stars , and radial velocities (RVs) for more than 7 million stars across its 1st, 2nd and early-3rd data releases (Gaia Collaboration et al. ????a,b). Combined, proper motion, position, and RV measurements provide the full 3-dimensional velocity vector for any given star. 3D stellar velocities are useful for calculating the relative space-motions of stars, and for revealing their Galactic orbits. The orbits of stars can be used to explore the secular dynamical evolution of the Galaxy, for example by studying vertical heating and radial migration (**?**). Stellar orbits can also help differentiate nascent and accreted stellar populations in the Milky Way's halo (**?**).

RV measurements, combined with proper motions, are extremely useful as they complete the full picture of 3D stellar velocity. However, RV measurements can only be calculated with a stellar spectrum – an observation requiring more photons than are needed for photometry or astrometry. RVs are therefore difficult to obtain for faint stars. Fortunately however, Gaia proper motion measurements are of such incredible precision that, even without an RV measurement, the 3D velocity of a star can still be inferred by marginalizing over radial velocity. This will often provide a velocity that is not equally well-constrained in every direction, *i.e.* the probability density function of a star's velocity will be an oblate spheroid in 3D. In the equatorial coordinate system, a star's velocity will be tightly constrained the RA and dec directions, and only constrained by the prior in the radial direction. Transforming to any other coordinate system, a star's velocity probability density function will change shape in a way that depends on its position.

There are several applications for which the 3D velocity of a star is useful, even if its velocity is not equally well-constrained in every direction. For example, Oh et al. (2017) used Gaia proper motions to identify comoving pairs and groups of stars and marginalized over missing RVs. In some cases, the velocities of stars in particular directions

are more useful than others, for example, the *vertical* velocities of stars ($v_{\mathbf{z}}$ or W) are often used to study the secular orbital heating of stars in the Milky Way's disk (*e.g.* Ting & Rix 2019; Beane et al. 2018; Yu & Liu 2018; **?**). Unless the radial velocity direction precisely coincides with the vertical axis of the Milky Way, *i.e.* a star lies along the Z axis of the Galactocentric coordinate system, we can still extract some $v_{\mathbf{z}}$ information from Gaia proper motions alone. Of course, the lower the Galactic latitude of a star, the better the constraint on its $v_{\mathbf{z}}$ will be (hence why the Kepler field, located at low latitude, is particularly useful for vertical velocity studies).

One of our main purposes in calculating the velocities of Kepler stars is to use Galactic kinematics to date them. The ages of stars, particularly GKM stars on the main sequence, are difficult to measure because their luminosities and temperatures evolve slowly (see Soderblom 2010, for a review of stellar ages). Empirical models that relate the magnetic activity or rotation periods of stars to their age can be used to infer the ages of some low-mass dwarfs (**?**), however, these empirical relations are often poorly calibrated for K and M dwarfs and old stars (**?**). Galactic kinematics provides an alternative, statistical dating method.

The star forming molecular gas clouds observed in the Milky Way have a low out-of-plane, or vertical, velocity (*e.g.* Stark & Brand 1989; Stark & Lee 2005; Aumer & Binney 2009; Martig et al. 2014; Aumer et al. 2016). In contrast, the vertical velocities of older stars are observed to be larger in magnitude on average (Strömberg 1946; Wielen 1977; Nordström et al. 2004; Holmberg et al. 2007, 2009; Aumer & Binney 2009; Casagrande et al. 2011; Ting & Rix 2019; Yu & Liu 2018). There are two possible explanations for this observed increase in velocity dispersion with age: either stars are born kinematically 'cool' and their orbits are heated over time via interactions with giant molecular clouds (see Sellwood 2014, for a review of secular evolution in the MW), or stars formed kinematically 'hotter' in the past (*e.g.* Bird et al. 2013). Either way, the vertical velocity dispersions of thin disk stars are observed to increase with stellar age. This behavior is codified by Age-Velocity dispersion Relations (AVRs), which typically express the relationship between age and velocity dispersion as a power law: $\sigma_v \propto t^\beta$, with free parameter, β (*e.g.* Holmberg et al. 2009; Yu & Liu 2018). These expressions can be used to infer the ages of groups of stars from their velocity dispersions. However, AVRs are usually calibrated in 3D Galactocentric velocities – most commonly in $v_{\mathbf{z}}$ or W. Regardless of the coordinate system, some transformation from proper motion in RA and dec is currently required to calculate the kinematic ages of stars.

AVRs are usually calibrated in Galactocentric velocity coordinates ($v_{\mathbf{x}}$, $v_{\mathbf{y}}$, $v_{\mathbf{z}}$ or UVW), and these velocities can only be calculated with full 6D positional and velocity information, however most Kepler rotators do not have RV measurements[1]. In Angus et al. (2020) we used the velocities of Kepler stars in the direction of Galactic latitude, $v_{\mathbf{b}}$ as a proxy for vertical velocity, $v_{\mathbf{z}}$ (the Kepler field is oriented at low Galactic latitude and $v_{\mathbf{b}}$ is therefore similar to $v_{\mathbf{z}}$). We used the velocity dispersions of stars as an age proxy, to explore the evolution of stellar rotation rates. In Lu et al. (2021) we used vertical velocity dispersion to calculate kinematic ages for Kepler stars with measured rotation periods using an AVR. Those vertical velocities were inferred by marginalizing over RVs using the method we describe in this paper.

This paper is laid out as follows. In section **??** we describe how we calculate the kinematic ages of Kepler stars from their positions, proper motions and parallaxes (and RVs where available). We also justify the choice of prior probability density function (PDF). In section **??** we use the 3D velocities of Kepler stars to calculate the kinematic ages of stars with marginal rotation period detections using the method of Lu et al. (2021). In section **??** we discuss the implications of our results and the applications and caveats of our velocities and velocity-inference code.

---

[1] Although RVs for most will be released in *Gaia* DR3

2. THE DATA

We used the Kepler-Gaia cross-matched catalog available at gaia-kepler.fun, which includes 194764 Kepler targets, cross-matched with Gaia targets within in a 1" radius. This catalog includes Gaia positions, parallaxes, and proper distances from Gaia EDR3 and RVs from Gaia DR2. It also includes distances inferred from Gaia EDR3 parallaxes (**?**). We crossmatched this catalog with the LAMOST DR5 catalog, also using a 1" radius and, where available, added APOGEE RVs from the DR16 stellar catalog (**?**). We removed stars with a Gaia parallax < 0, parallax signal-to-noise ratio < 10, or Gaia astrometric excess noise > 5. After applying these cuts our total number of targets was 178,000 stars: 28,112 with RVs from Gaia DR2, 37,567 from LAMOST DR5, and XXX from APOGEE DR16. In total, 58,397 stars in our sample have RVs from *either* Gaia, LAMOST, or APOGEE, 12,282 have RVs from two sources, and XXX from all three. The APOGEE survey has a higher spectral resolution than Gaia, which is higher than LAMOST. The median RV uncertainty for stars in our sample is around 0.1 km/s for APOGEE RVs, 1 km/s for Gaia RVS, and 4 km/s for LAMOST RVs. In cases where stars had two or more available RV measurements, we adopted APOGEE RVs as a first priority, followed by Gaia, then LAMOST.

Although RVs are available for more than one in three stars in this Kepler sample, most stars with RVs are bright. Very few of the coolest stars have RV measurements because of the selection functions of spectroscopic surveys. *Gaia* DR2 only includes RVs for stars brighter than around 13th magnitude, and *LAMOST* only provides RVs for Kepler stars brighter than around 17th magnitude in *Gaia G*-band. Ruth, check the actual LAMOST selection function. Figure **??** shows the apparent magnitude and temperature distributions of the stars in our sample, with and without RVs. This figure reveals the combined selection functions of the Gaia, LAMOST and APOGEE RV surveys and shows that faint stars have fewer RV measurements than bright ones.   Given that rotational evolution is particularly

Figure 1. The distribution of apparent Gaia magnitudes for stars in our sample with and without RV measurements from Gaia, LAMOST and APOGEE.
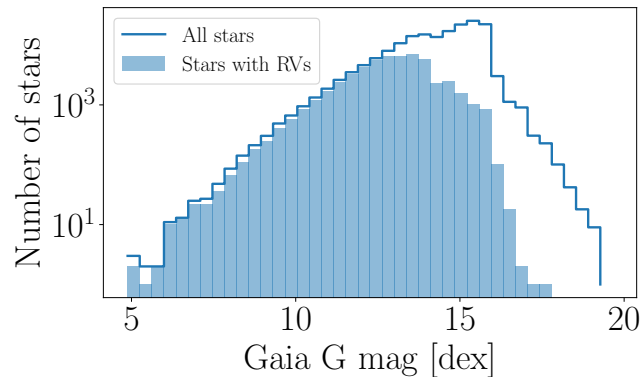
poorly understood for M dwarfs, the cool stars with missing RVs are arguably the most interesting. To fill-in the low-temperature regime, we inferred velocities for stars without RV measurements, by marginalizing over missing RVs.

Figure 2. The color-temperature diagram of stars in the Kepler field with (left) and without (right) RVs provided by Gaia, LAMOST and APOGEE. The stars with RVs are generally hotter and more luminous than those without RVs, and include a large number of red clump stars and red giant branch stars. Stars without RVs are mostly concentrated on the main sequence.
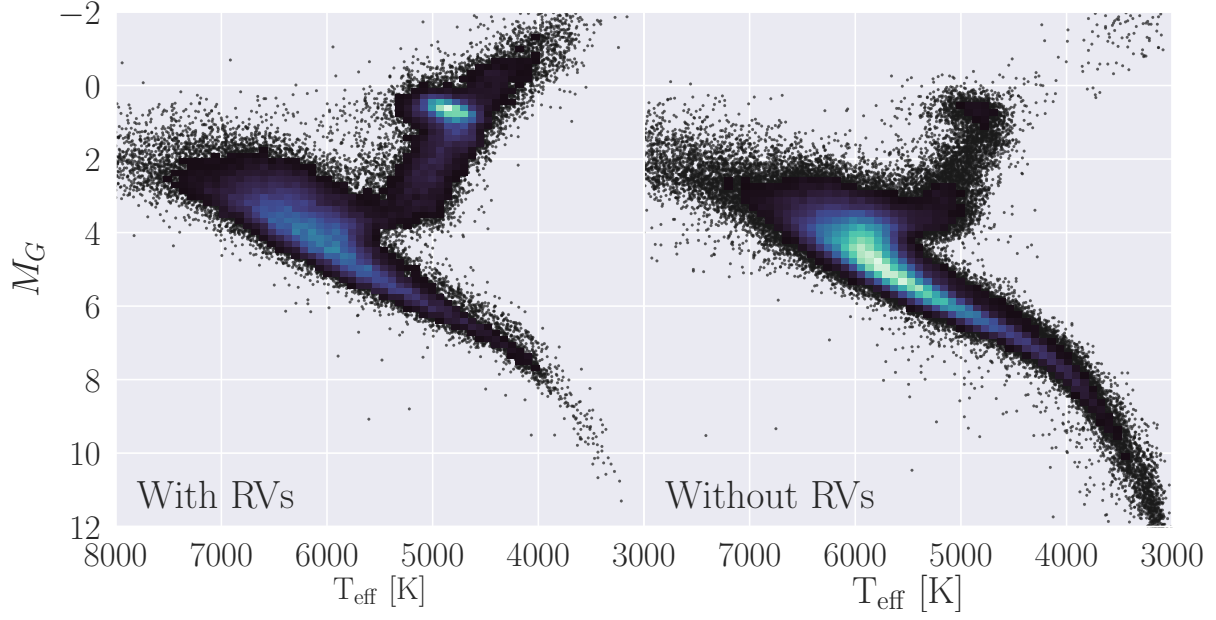
3. STELLAR VELOCITIES

In this section we describe how we calculated full 3D velocities for the field stars in our sample, which were then used to calculate kinematic ages using the method described in Lu et al. (2021).

Most AVRs are calibrated using velocities in Galactocentric coordinates, $v_\mathbf{x}$, $v_\mathbf{y}$ and $v_\mathbf{z}$, which can only be calculated with full 6-D position and velocity information, *i.e.* proper motions, position and radial velocity. In Angus et al. (2020) we explored rotational evolution using velocity dispersion as an age proxy, however we used velocity in the direction of Galactic latitude, $v_\mathbf{b}$, instead of $v_\mathbf{z}$. This is because $v_\mathbf{b}$ can be calculated without an RV measurement but is a close approximation to $v_\mathbf{z}$ for Kepler stars due to the orientation of the Kepler field. The Kepler field lies at low Galactic latitudes, ($\sim 5-20°$), so the **z**-direction is similar to the **b**-direction for Kepler stars. However, even at such low latitudes, kinematic ages calculated with $v_\mathbf{b}$ instead of $v_\mathbf{z}$ are likely to be systematically larger because of mixing between $v_\mathbf{z}$, $v_\mathbf{x}$ and $v_\mathbf{y}$. A direct measurement or precise estimate of $v_\mathbf{z}$ is necessary to calculate accurate kinematic ages. Less than 1 in 3 stars in our sample of Kepler rotators have a directly measured RV available, and for these $\sim$11,000 stars we calculated vertical velocities, $v_\mathbf{z}$, using the `coordinates` library of `astropy` (Astropy Collaboration et al. 2013; Price-Whelan et al. 2018). For the remaining stars we *inferred* their vertical velocities by marginalizing over their RVs.

3.1. *Inferring 3D velocities (marginalizing over missing RV measurements)*

For each star in our sample without an RV measurement, we inferred $v_\mathbf{x}$, $v_\mathbf{y}$, and $v_\mathbf{z}$ from the 3D positions (right ascension, α, declination, δ, and parallax, π) and 2D proper motions (μ_α and μ_δ) provided in the *Gaia* DR2 catalog (Brown et al. 2011). We also simultaneously inferred distance, (instead of using inverse-parallax), to model velocities (see *e.g.* Bailer-Jones 2015; Bailer-Jones et al. 2018).

Using Bayes rule, the posterior probability of the velocity parameters given the Gaia data can be written:

$$p(\mathbf{v_{xyz}}, D|\mu_\alpha, \mu_\delta, \alpha, \delta, \pi) = p(\mu_\alpha, \mu_\delta, \alpha, \delta, \pi|\mathbf{v_{xyz}}, D)p(\mathbf{v_{xyz}})p(D), \tag{1}$$

where D is distance and $\mathbf{v_{xyz}}$ is the 3D vector of velocities. To evaluate the likelihood function, our model predicted observable data from model parameters, *i.e.* it converted $v_\mathbf{x}$, $v_\mathbf{y}$ $v_\mathbf{z}$ and D to μ_α, μ_δ and π. In the first step of the model evaluation, cartesian coordinates, **x**, **y**, and **z** were calculated from α and δ measurements and D ($1/\pi$) for each star, by applying a series of matrix rotations, and a translation to account for the Solar position. The cartesian Galactocentric velocity parameters, $v_\mathbf{x}$, $v_\mathbf{y}$, and $v_\mathbf{z}$, were then converted to equatorial coordinates, μ_α and μ_δ, via another rotation.

As mentioned previously, the specific positioning of the Kepler field (at low Galactic latitude) allows $v_\mathbf{z}$ to be well-constrained from proper motion measurements alone. This also happens to be the case for $v_\mathbf{x}$, because the direction of the Kepler field is almost aligned with the **y**-axis of the Galactocentric coordinate system and is almost perpendicular to both the **x** and **z**-axes (see figure 3). For this reason, the **y**-direction is similar to the radial direction for observers near the Sun, so $v_\mathbf{y}$ will be poorly constrained for Kepler stars without RV measurements. On the other hand, $v_\mathbf{x}$ and $v_\mathbf{z}$ are almost perpendicular to the radial direction and can be precisely inferred with proper motions alone.

3.2. *The prior*

The prior distribution over distance and velocities was constructed from the data. We calculated the means and covariances of the $v_\mathbf{x}$, $v_\mathbf{y}$, $v_\mathbf{z}$ and $\ln(D)$ distributions of stars *with measured RVs* and then used these means and covariances to construct a multivariate Gaussian prior over the parameters for stars *without* RVs. Velocity outliers greater than 3-σ were removed before calculating the means and covariances of the distributions. The 2-dimensional ln-distance and velocity distributions are displayed in figure 4, with 2-σ contours shown in blue.

Our goal was to infer the velocities of stars *without* RV measurements using a prior calculated from stars *with* RV measurements. However, stars with and without RVs are likely to be different populations, with parameters that depend on the *Gaia* and *LAMOST* selection functions. In particular, stars without RV measurements are more likely to be fainter, cooler, and further away. For this reason, a prior based on the velocity distributions of stars with RVs will not necessarily reflect the velocities of those without. However, given that $v_\mathbf{x}$ and $v_\mathbf{z}$ are strongly informed by proper motion measurements, and therefore likely to be relatively prior-insensitive, the prior may not impact our final vertical velocity, and subsequent kinematic ages, significantly. Remember, we are mainly interested in the $v_\mathbf{z}$ parameter because *vertical* velocity dispersion is a well-studied age indicator.

Figure 3. **x**, **y** and **z** positions of stars observed by Kepler, showing the orientation of the Kepler field. The direction of the field is almost aligned with the **y**-axis and almost perpendicular to the **x** and **z**-axes, which is why $v_{\mathbf{x}}$ and $v_{\mathbf{z}}$ can be tightly constrained for Kepler stars without RVs, but $v_{\mathbf{y}}$ cannot.
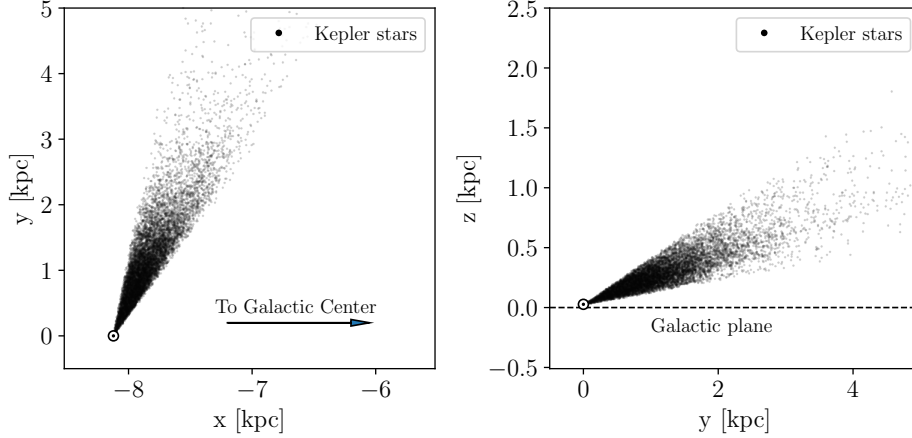
Figure 4. The 2D velocity and distance distributions for stars with RV measurements, used to construct a multivariate Gaussian prior over velocity and distance parameters for stars *without* RVs. 2-σ contours are shown in blue.
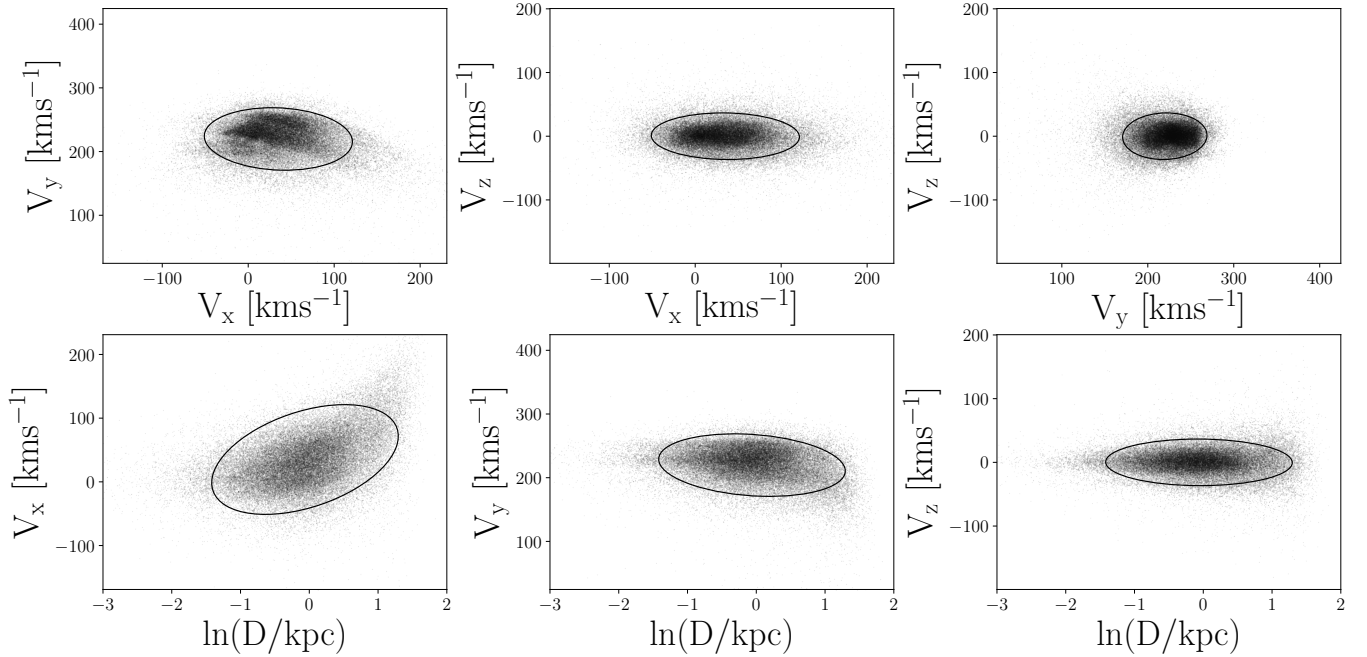
We tested the influence of the prior on the velocities we inferred. One of the main features of the *Gaia* and *LAMOST* RV selection functions is brightness: *Gaia* DR2 RVs are only available for stars brighter than around 13th magnitude, and *LAMOST* RVs for stars brighter than around 17th magnitude. Ruth, check the actual LAMOST selection function. For this reason, we tested priors based on stellar populations with different apparent magnitudes. Three priors were tested: one calculated from the velocity distributions of the brightest half of the RV sample (*Gaia G*-band apparent magnitude < 13.9), one from the faintest half ($G > 13.9$), and one from all stars with RVs. Figure 5 shows the distributions of the faint (blue) and bright (orange) halves of the RV sample as kernel density estimates (KDEs). The distributions are different because bright stars are more massive, younger, and closer to the Sun on average than faint stars. As a result, these stars occupy slightly different Galactic orbits. The Gaussian fits to these distributions, which

were used as prior PDFs, are shown in figure **??** as dashed, colored lines. The Gaussian fit to *all* the data, both bright and faint, is shown as a black solid line. The means of the faint and bright distributions differed by 6 kms^{-1}, 5 kms^{-1}, 1 kms^{-1} and 0.21 kpc, for $v_\mathbf{x}$ $v_\mathbf{y}$, $v_\mathbf{z}$ and $\ln(D)$, respectively. The $v_\mathbf{x}$, $v_\mathbf{y}$, and distance distributions of these stars are strongly dependent on brightness. However, the $v_\mathbf{z}$ distribution does not vary significantly with stellar brightness. Since $v_\mathbf{z}$ is the only velocity we actually used to infer kinematic ages, this indicates that the choice of prior does not strongly impact our final results. To confirm this, we tested the influence of the prior on the parameters.

Figure 5. Velocity and distance distributions of faint (blue) and bright (orange) stars with RVs, shown as KDEs. Gaussian fits to these distributions are shown as dashed lines in corresponding colors. The solid black line shows the Gaussian fit to all data (bright and faint combined) and is the prior we ended up using in our model.
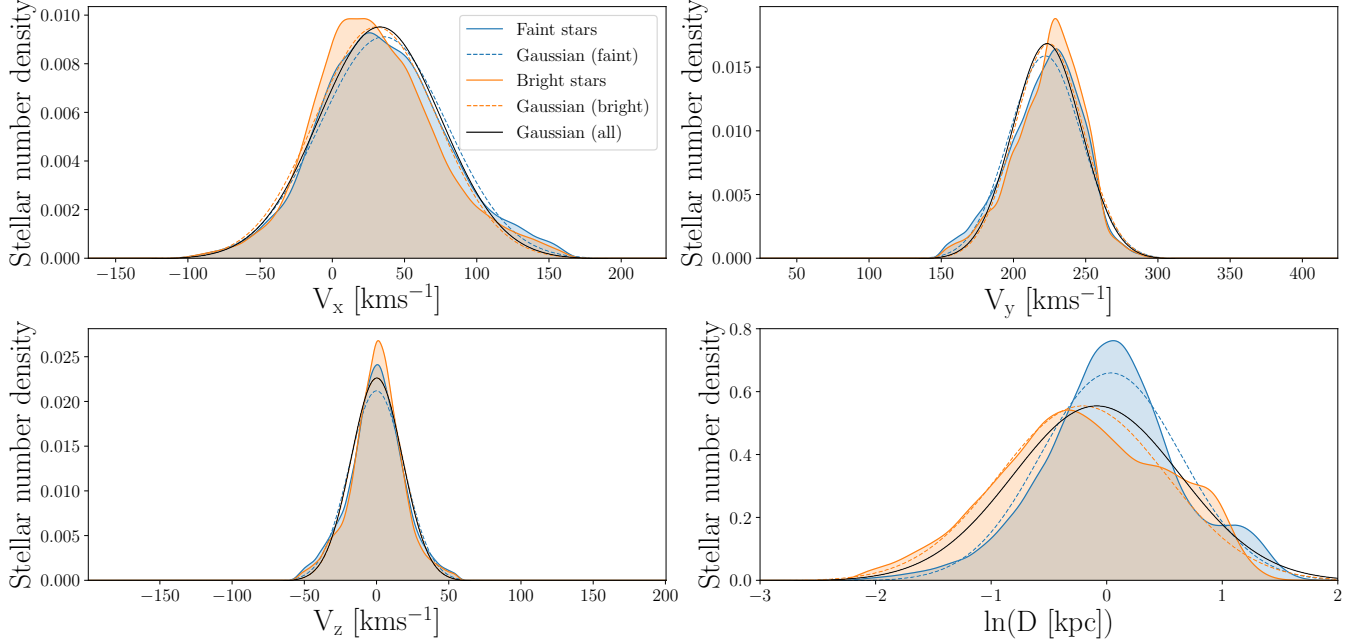

We inferred the velocities of 3000 stars chosen at random from the *Gaia-LAMOST* RV sample using each of these three priors and compared the inferred velocity distributions. If the inferred velocities were highly prior-dependent, the resulting distributions, obtained from different priors, would look very different. The results of this test are shown in figure **??**. From left to right, the three panels show the distributions of inferred $v_\mathbf{x}$, $v_\mathbf{y}$, and $v_\mathbf{z}$. The blue dashed line shows a KDE, representing the distributions of velocities inferred using the prior calculated from the faint half of the RV sample. Similarly, the solid orange line shows the distribution of inferred velocities using the prior calculated from the bright half of the RV sample, and the solid black line shows the results of the prior calculated from *all* stars with measured RVs.

The median values of the $v_\mathbf{y}$ distributions, resulting from the faint and bright priors, differ by around 4 kms^{-1}. This is similar to the difference in means of the faint and bright populations (5 kms^{-1}, as quoted above). The inferred $v_\mathbf{x}$ and $v_\mathbf{z}$ distributions differ by 2 kms^{-1} and 0.3 kms^{-1}, respectively. Regardless of the prior choice, the $v_\mathbf{x}$ and $v_\mathbf{z}$ distributions are similar because velocities in the $\mathbf{x}$ and $\mathbf{z}$-directions are not strongly prior dependent: they are tightly constrained with proper motion measurements alone. However, the distribution of inferred $v_\mathbf{y}$ velocities *does* depend on the prior. This is because the $\mathbf{y}$-direction is close to the radial direction for Kepler stars (see figure 3), and $v_\mathbf{y}$ cannot be tightly constrained without an RV measurement.

Although this test was performed on stars with RV measurements, which are brighter overall than the sample of stars without RVs (*e.g.* figure **??**), figure **??** nevertheless shows that $v_\mathbf{x}$ and $v_\mathbf{z}$ are not strongly prior-dependent. In this work we are only concerned with $v_\mathbf{z}$, as we only use *vertical* velocity dispersion as an age indicator. The difference in the dispersions of $v_\mathbf{z}$ velocities, calculated with the three different priors tested above was smaller than 0.5 kms^{-1}.

Figure 6. The distributions of velocity and distance parameters, inferred using three different priors. The orange line is a KDE that represents the distribution of parameters inferred with a Gaussian prior, estimated from the bright half of the RV sample ($G < 13.9$). The blue dashed line shows the results from a prior estimated from the faint half of the RV sample ($G > 13.9$. The black line shows the results from a prior calculated from all stars with RV measurements and is the prior we adopt in our final analysis.
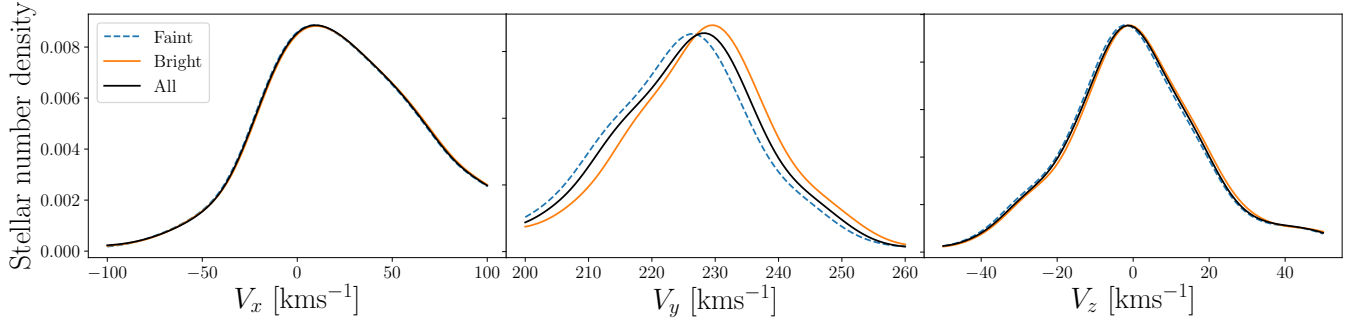
We therefore conclude that vertical velocity dispersion is relatively insensitive to prior choice, and we adopt a prior calculated from the distributions of all stars with RV measurements (black Gaussians in figure **??**).

For each star in the Kepler field, we explored the posteriors of the four parameters, $v_{\mathbf{x}}$, $v_{\mathbf{y}}$, $v_{\mathbf{z}}$, and $\ln(D)$ using the *PyMC3* No U-Turn Sampler (NUTS) algorithm, and the `exoplanet` *Python* library (citations). We tuned the *PyMC3* sampler for 1500 steps, with a target acceptance fraction of 0.9, then ran four chains of 1000 steps for a total of 4000 steps. Using PyMC3 made the inference procedure exceptionally fast – taking just a few seconds per star on a laptop. Check what convergence criteria you should use, or justify these choices.

4. RESULTS

4.1. *Inferred velocities*

To validate our method, we inferred velocities for stars in our sample with measured RVs and compared those inferred values with velocities calculated directly from 6D position, proper motion, and RV measurements. Figure **??** shows the $v_\mathbf{x}$, $v_\mathbf{y}$ and $v_\mathbf{z}$ velocities we inferred, for 3000 stars chosen at random, compared with those calculated from measured RVs.

Figure 7. Vertical velocities calculated with full 6D information vs vertical velocities inferred without RVs, for 3000 McQuillan et al. (2014) stars with *Gaia* RV measurements.
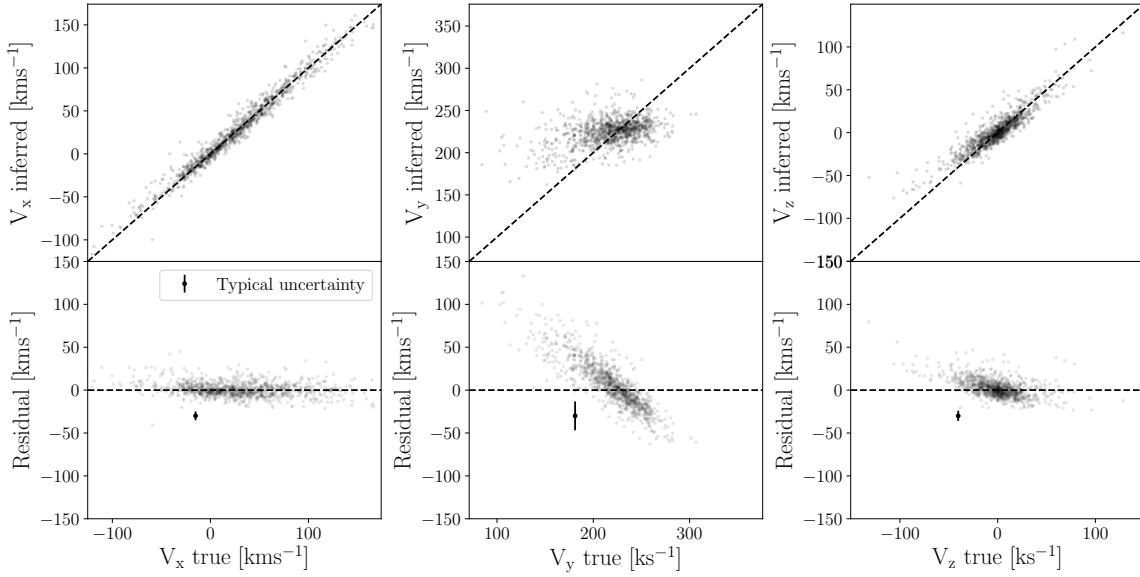
The three velocity components, $v_\mathbf{x}$, $v_\mathbf{y}$ and $v_\mathbf{z}$ were recovered with differing levels of precision: $v_\mathbf{x}$ and $v_\mathbf{z}$ are inferred more precisely than $v_\mathbf{y}$. This is because of the orientation of the Kepler field, shown in figure 3. Slight inaccuracies seen in the residual panels for $v_\mathbf{x}$ and $v_\mathbf{z}$ are caused by .... Quote some summary statistics.

Table **??** contains the inferred 3D velocities of stars in our sample, in addition to their positional and velocity information from Gaia EDR3, LAMOST DR5 and APOGEE DR16. A sample of this table is displayed here, and the full machine-readable table is available online.

5. CONCLUSION

This paper describes a method for inferring the 3D velocities of stars by marginalizing over missing radial velocity measurements. We focused on stars in the Kepler field, because of its potential for studying stellar evolution via kinematic age-dating, and because of its particular orientation. Located at low Galactic latitude, the Kepler field is almost aligned with the y-axis of the Galactocentric coordinate system. This means that 2D Gaia proper motion measurements alone are sufficient to tightly constrain the $v_{\mathbf{x}}$ and $v_{\mathbf{z}}$ velocities of Kepler stars. Without RV measurements however, the $v_{\mathbf{y}}$ velocities of Kepler stars are poorly constrained. However, given that many age-velocity dispersion relations (AVR) are calibrated in *vertical* velocity, $v_{\mathbf{z}}$ is the main parameter of interest for kinematic age-dating.

We compiled crossmatches of the Kepler, Gaia EDR3, LAMOST DR5 and APOGEE DR16 catalogs. Gaia EDR3 provided parallaxes, positions and proper motions for the stars in our sample, and Gaia DR2 provided RVs for XXX stars. LAMOST DR5 provided XXX RVs for stars in our sample, and APOGEE DR16 provided XXX. Of the three spectroscopic surveys, APOGEE has the highest resolution, followed by Gaia, then LAMOST, so we adopted RVs in that priority-order where stars had multiple RV measurements available.

We calculated $v_{\mathbf{x}}$, $v_{\mathbf{y}}$, and $v_{\mathbf{z}}$ for the XXX stars in our sample with RVs using `astropy`. For the remaining XXX stars, we *inferred* $v_{\mathbf{x}}$, $v_{\mathbf{y}}$, $v_{\mathbf{z}}$, and distance while marginalizing over RV. Our prior was a 4D Gaussian in $v_{\mathbf{x}}$, $v_{\mathbf{y}}$, $v_{\mathbf{z}}$ and ln(distance), which was based on the distribution of stars in our sample *with* RVs. Since the populations of stars with and without RVs in the Kepler field are somewhat different – stars *with* RVs are generally brighter than stars without – we tested the sensitivity of our results to the prior. We split the subsample of stars with measured RVs into two further subgroups: stars brighter and stars fainter than 13th magnitude in Gaia G-band (13th being the median magnitude of the Kepler stars with RVs). Priors were constructed from the faint and bright halves of the sample and used to infer the velocities of 1000 stars randomly selected from the total RV sample. Upon examination, we found the final inferred velocities were similar, irrespective of the prior. As expected, $v_{\mathbf{x}}$ and $v_{\mathbf{z}}$ depend very little on the prior but $v_{\mathbf{y}}$ has a stronger prior-dependence because it is difficult to constrain without an RV for Kepler stars. A caveat of our inferred velocities is therefore that the $v_{\mathbf{y}}$ velocities may not be accurate for faint stars in the Kepler field.

We provide a table of $v_{\mathbf{x}}$, $v_{\mathbf{y}}$, $v_{\mathbf{z}}$, and ln(distance) for a total of XXX stars observed by Kepler. This table also contains the positional and velocitiy information from Gaia DR2, Gaia EDR3, LAMOST DR5, and APOGEE DR16.

REFERENCES

Angus, R., Beane, A., Price-Whelan, A. M., et al. 2020, AJ, 160, 90, doi: 10.3847/1538-3881/ab91b2

Astropy Collaboration, Robitaille, T. P., & Tollerud *et al*, E. J. 2013, A&A, 558, A33, doi: 10.1051/0004-6361/201322068

Aumer, M., Binney, J., & Schönrich, R. 2016, MNRAS, 462, 1697, doi: 10.1093/mnras/stw1639

Aumer, M., & Binney, J. J. 2009, MNRAS, 397, 1286, doi: 10.1111/j.1365-2966.2009.15053.x

Bailer-Jones, C. A. L. 2015, PASP, 127, 994, doi: 10.1086/683116

Bailer-Jones, C. A. L., Rybizki, J., & Fouesneau *et al*, M. 2018, AJ, 156, 58, doi: 10.3847/1538-3881/aacb21

Beane, A., Ness, M. K., & Bedell, M. 2018, ApJ, 867, 31, doi: 10.3847/1538-4357/aae07f

Bird, J. C., Kazantzidis, S., & Weinberg *et al*, D. H. 2013, ApJ, 773, 43, doi: 10.1088/0004-637X/773/1/43

Brown, T. M., Latham, D. W., & Everett *et al*, M. E. 2011, AJ, 142, 112, doi: 10.1088/0004-6256/142/4/112

Casagrande, L., Schönrich, R., & Asplund *et al*, M. 2011, A&A, 530, A138, doi: 10.1051/0004-6361/201016276

Gaia Collaboration, Prusti, T., de Bruijne, J. H. J., et al. ????a

Gaia Collaboration, Brown, A. G. A., Vallenari, A., et al. ????b

Holmberg, J., Nordström, B., & Andersen, J. 2007, A&A, 475, 519, doi: 10.1051/0004-6361:20077221

—. 2009, A&A, 501, 941, doi: 10.1051/0004-6361/200811191

Lu, Yuxi, Angus, R., et al. 2021, arXiv e-prints, arXiv:2102.01772. https://arxiv.org/abs/2102.01772

Martig, M., Minchev, I., & Flynn, C. 2014, MNRAS, 443, 2452, doi: 10.1093/mnras/stu1322

McQuillan, A., Mazeh, T., & Aigrain, S. 2014, ApJS, 211, 24, doi: 10.1088/0067-0049/211/2/24

Nordström, B., Mayor, M., & Andersen *et al*, J. 2004, A&A, 418, 989, doi: 10.1051/0004-6361:20035959

Oh, S., Price-Whelan, A. M., Hogg, D. W., Morton, T. D., & Spergel, D. N. 2017, AJ, 153, 257, doi: 10.3847/1538-3881/aa6ffd

Price-Whelan, A. M., Sipőcz, B. M., & Günther *et al*, H. M. 2018, AJ, 156, 123, doi: 10.3847/1538-3881/aabc4f

Sellwood, J. A. 2014, Reviews of Modern Physics, 86, 1, doi: 10.1103/RevModPhys.86.1

Soderblom, D. R. 2010, ARA&A, 48, 581, doi: 10.1146/annurev-astro-081309-130806

Stark, A. A., & Brand, J. 1989, ApJ, 339, 763, doi: 10.1086/167334

Stark, A. A., & Lee, Y. 2005, ApJL, 619, L159, doi: 10.1086/427936

Strömberg, G. 1946, ApJ, 104, 12, doi: 10.1086/144830

Ting, Y.-S., & Rix, H.-W. 2019, ApJ, 878, 21, doi: 10.3847/1538-4357/ab1ea5

Wielen, R. 1977, A&A, 60, 263

Yu, J., & Liu, C. 2018, MNRAS, 475, 1093, doi: 10.1093/mnras/stx3204